ELSEVIER

Polymer 42 (2001) 1017–1022

polymer

www.elsevier.nl/locate/polymer

# Surface characterization of blood compatible amphiphilic graft copolymers having uniform poly(ethylene oxide) side chains

Shengrong Guo[a,*], Liangjun Shen[b], Linxian Feng[c]

[a]*Department of Pharmaceutics, Shanghai Medical University, 138 Yixueyuan Road, Shanghai 200032, People's Republic of China*
[b]*Institute of Organic Chemistry, Anhui Normal University, 241000, People's Republic of China*
[c]*Department of Polymer Science and Engineering, Zhejiang University, 310027, People's Republic of China*

Received 24 February 2000; received in revised form 5 June 2000; accepted 27 June 2000

**Abstract**

The surface characterization of poly(methyl methacrylate)-*graft*-poly(ethylene oxide) (PMMA-*g*-PEO) was investigated by XPS and contact-angle measurement, and its in vitro blood compatibility was assessed by plasma recalcification time measurement. The surface and bulk composition of different PMMA-*g*-PEO graft copolymer showed that PMMA segments were always enriched at the copolymer–air interface, but surface enrichment of PEO segments could occur in films of copolymers with longer PEO side chain ($M_n$ of PEO, 3200) and a higher bulk PEO content. Contact-angle studies indicated that the surface hydrophilicity increased as the surface PEO content increased. The contact angles of water on the copolymer decreased linearly with contact time until they reached a balance value $\theta_e$ or 0, and the relationship between $\theta$ (from the static contact angle, $\theta_s$ to $\theta_e$) and contact time($t$) can be expressed by: $\theta = -kt$. The proportionality constant $k$ and $\Delta\theta$ ($\theta_s - \theta_e$) depended on the bulk structural parameters (the bulk composition and PEO side chain length). The microphase-separated structure of copolymers was also observed by transmission electron microscopy (TEM). The relationship between the surface properties of PMMA-*g*-PEO graft copolymer and its blood compatibility was addressed. © 2000 Published by Elsevier Science Ltd.

*Keywords*: PMMA-*g*-PEO; Contact angle; XPS

## 1. Introduction

During the past few decades, the design, synthesis and characterization of blood-compatible polymers have become one of the most important research areas in polymer sciences. Because blood coagulation can be triggered by a material surface, the surface properties of such materials and blood compatibility of these surfaces have received much attention [1–3].

PEO-based biomedical polymers have been shown as good blood-compatible materials [4–8]. However, surface properties and their relationship with biocompatibility, only in block copolymers and polymer blends, have been studied intensively [9–12]. Surface properties of graft copolymers with PEO side chains and their relationship with the bulk structure have received little attention. This interesting problem merits detailed studies.

PMMA-*g*-PEO is an amphiphilic graft copolymer with uniform PEO side chains and has a definite structure, making it a good model polymer for studying the relationship between the surface properties and bulk structural parameters (bulk composition and PEO grafts). This paper will report our studies of the surface characterization and in vitro blood compatibility assessment of PMMA-*g*-PEO.

## 2. Experimental

### 2.1. Synthesis and bulk characterization

#### 2.1.1. Materials

α-Methacrylic acid (MMA) was purified by distillation under reduced pressure. MAA was dried with silica gel overnight and distilled under reduced pressure. Ethylene oxide (EO) was treated first with KOH and then with $CaH_2$, followed by distillation. Azobisisobutyronitrile (AIBN) was recrystallized from ethanol. Toluene was dried by distillation over $CaH_2$. Phenol was purified by distillation. α-methacryloyl chloride (MAC) was synthesized from α-methacrylic acid and phosphorus trichloride and purified by twice distillation over CuCl. Potassium phenolate was synthesized from phenol and potassium hydroxide.

* Corresponding author. Current address: School of Pharmacy; Shanghai Jiao Tong University, 1954 Hua Shan Road, Shanghai 20030, People's Republic of China.
*E-mail address:* guosr@public8.sta.net.cn (S. Guo).

0032-3861/01/$ - see front matter © 2000 Published by Elsevier Science Ltd.
PII: S0032-3861(00)00472-9

Table 1
Characteristics of PMMA-*g*-PEO ($M_n$ of PEO macromonomer in the copolymer A, B, C, D or E is 1650; $M_n$ of PEO macromonomer in the copolymer F, G, H, I or J is 3200)

| Samples | A | B | C | D | E | F | G | H | I | J |
|---|---|---|---|---|---|---|---|---|---|---|
| $M_n \times 10^{-4}$ | 6.21 | 6.95 | 7.06 | 8.39 | 8.36 | 7.75 | 7.82 | 8.10 | 8.26 | 7.55 |
| $M_w/M_n$ | 1.8 | 1.8 | 1.9 | 2.1 | 2.1 | 1.8 | 1.8 | 2.0 | 1.9 | 1.8 |
| EO (mol%) | 34.7 | 49.1 | 56.8 | 61.1 | 68.8 | 38.0 | 49.2 | 56.5 | 65.2 | 74.1 |

*2.1.2. Synthesis of PEO macromonomers*

Anionic polymerization was conducted at 70°C in a rigorously clean high-pressure reactor equipped with a stirrer and a pressure gauge, toluene as solvent and EO were injected into the reactor, and a calculated amount of potassium phenolate was added to initiate the reaction. The conversion of EO is judged to be complete when the pressure value dropped to zero on the gauge, the reaction was terminated by injecting a twofold excess of methacryloyl chloride into the system and kept at 30°C for 6 h. The product was precipitated and washed with ethyl ether. The precipitate was dissolved in 2% HCl aqueous solution and extracted with chloroform, the chloroform extractives was reprecipitated with ethyl ether, filtered and dried in vacuum to constant weight.

*2.1.3. Copolymerization of PEO macromonomer with MMA*

A certain amount of PEO macromonomer was dissolved in toluene and then MMA and AIBN were added. Copolymerization was carried out at 65°C with stirring under $N_2$ for 10 h. The reaction was terminated with hydroquinone. The product was precipitated with ethyl ether. The crude product was extracted with water to remove residual PEO macromonomer, and then with ethyl ether/acetone (5/2, v/v) to remove any homopolymer of MMA.

*2.1.4. Bulk characterization*

The molecular characteristics of PMMA-*g*-PEO are shown in Table 1. The molecular weights of PMMA-*g*-PEO and PEO macromonomers were measured by gel permeation chromatography (GPC) and vapor phase osmometer (VPO), respectively, and the copolymer composition was determined by $^1$H NMR. $^1$H NMR spectra were recorded on JEOL FX-90Ω spectrometer, using $CDCl_3$ or $CD_3SOCD_3$ as solvent and tetramethyl silane (TMS) as internal standard. The molar masses and molar mass distributions were investigated with Knaner VPO apparatus, using toluene as solvent and bibenzoyl as standard, 37°C and Waters-208 type apparatus, using tetrahydrofuran as eluent.

*2.2. Thin polymer film preparation*

Thin polymer films for XPS and contact-angle measurement were cast from dilute solution of PMMA–PEO in chloroform (1%) on clean glass plates. The obtained films were dried in vacuum at ambient temperature for three days. For each polymer sample, several replica films were prepared for XPS and contact-angle measurement.

*2.3. X-ray photoelectron spectroscopy*

Spectra were recorded on an ESCALAB MARK II spectrometer by using Al*K* exciting radiation. The basic pressure in the measurement chamber was kept around $10^{-8}$ torr. The value of 285.0 eV of the hydrocarbon $C_{1s}$ core level was used as a calibration for the absolute energy scale. Overlapping peaks were resolved into their individual components by use of the software dedicated in the XPS spectrometer. The detailed deconvolutions were based on the knowledge of binding energies and full widths at half maximum (FWHMs) from studies of corresponding homopolymers.

*2.4. Contact angle measurement*

The measurement of contact angle was performed at 20°C in the range of 0.5–20 min by sessile drop method, employing a contact-angle measurement apparatus (type JY-82, made in Chengde Instrument Factory, Chengde city, People's Republic of China). The static contact angle ($\theta_s$) was measured at contact time $t = 30$ s. Drops of liquid (1.5 ~ 2.0 mm diameter) were prepared with a microsyringe and were dropped onto the surface of polymer films.

*2.5. Transmission electron microscopy (TEM)*

TEM was performed on ultrathin films cast from 0.05% w/v polymer solutions in $CHCl_3$ on the surface of water. Grids were placed on the top of the film and the grids with film were collected from the water surface using a glass slide. Samples (grids with ultrathin films) were exposed to vapors of $O_sO_4$ and observed and micrographed with a transmission electron microscope (JEM 200CX, JEOL).

*2.6. In vitro blood compatibility assessment of PMMA-g-PEO*

Interior surfaces of small glass tubes (12 × 75 mm) were cast with 1% w/v solution of PMMA-*g*-PEO in chloroform, and dried three days in vacuum at ambient temperature. Then the recalcification time (RT) of fresh human platelet-rich plasma on the coated surfaces were measured. For each sample, the mean of six separate RT values was obtained and used to evaluate the blood compatibility of PMMA-*g*-PEO

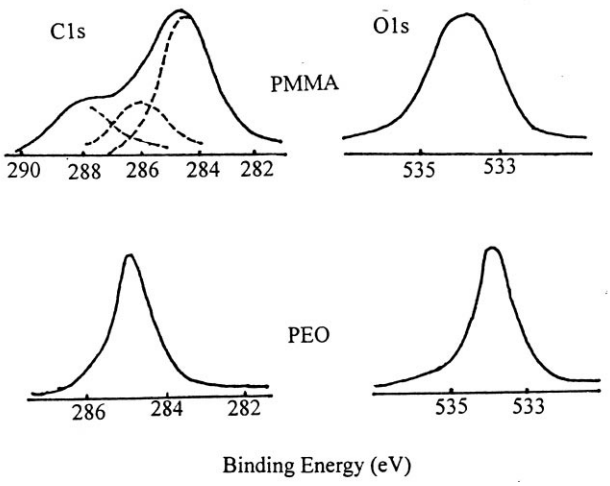


Fig. 1. The XPS core level spectra of PMMA and PEO.

graft copolymers. The films coated on the interior surfaces of small glass tubes were treated by immersion of the glass tubes in twice-distilled water for 30 min., then the tubes were removed from water. After surface water treatment, the RT was measured immediately.

## 3. Results and discussion

### 3.1. Surface chemical composition

#### 3.1.1. Homopolymers

To interpret the graft copolymer data, it is necessary to study the component homopolymers, PMMA and PEO, and determine their absolute and relative binding energies and relative peak intensities. The XPS core-level spectra for PMMA and PEO are shown in Fig. 1, and the experimental binding energies and peak intensity ratios are tabulated in Table 2.

The $C_{1s}$ spectrum for PMMA homopolymer consists of a doublet with an apparent shoulder on the higher binding-energy side of the main backbone carbon peak. The peak with the highest binding energy, corresponds to the carbonyl carbons, and the peak appearing as a shoulder on the main backbone carbon peak shifted by about 1.6 eV represents the attached singly-bonded oxygen. The relative peak intensity ratio for the $C_{1s}$ core levels is 59:21:19, and is very consistent with the ratio of the main backbone carbons, carbonyl, and ether carbons. In observing the $O_{1s}$ levels for PMMA, it is apparent that the overall band profiles arise from two peaks of equal intensity, separated by about 1.4 eV, assigned to the carbonyl- and ether-type oxygens. The spectra for PEO show a single peak for the $C_{1s}$ levels at 286.5 eV, in reference to hydrocarbon, which is at 285 eV, and a single peak for the $O_{1s}$ core levels at 532.9 eV. These results show that the peak at about 286.5 eV is attributable to the carbons singly bonded to oxygen of both of PMMA and PEO segments in the $C_{1s}$ spectrum for PMMA-*g*-PEO, and allow for an analysis of the surface composition of the PMMA-*g*-PEO graft copolymers. The surface composition can be calculated through the deconvolution of the $C_{1s}$ spectra for the copolymers and from the signal intensities for each of the components.

Table 2
Experimental binding energies, peak intensity ratios, and FWHMs for the reference homopolymers, PMMA and PEO

| Sample | | Binding energies (ev) | FWHMs (ev) | Peak intensity ratios |
|---|---|---|---|---|
| PMMA | $C_{1s}$ | 285.0 | 2.21 | 59 |
| | | 286.6 | 1.99 | 20 |
| | | 288.8 | 2.26 | 21 |
| | $O_{1s}$ | 532.9 | 2.50 | 51 |
| | | 534.5 | 2.62 | 49 |
| PEO | $C_{1s}$ | 286.7 | 2.08 | |
| | $O_{1s}$ | 532.9 | 2.11 | |

#### 3.1.2. PMMA-g-PEO copolymers

The relationship between the surface and bulk composition of the graft copolymers is shown in Fig. 2. Clearly, the bulk composition and graft chain length greatly influenced the surface composition. In general, the surface concentration of PMMA was higher than its bulk concentration. This is because the surface free energy of PMMA is lower than that of PEO. In air, a surface is preferentially enriched with a lower surface free energy component.

For the copolymers with the same PEO side chain length, the surface concentration of PEO component increased as its bulk concentration increased. For the copolymers with long PEO side chains ($M_n$ of PEO, 3200), a surface enrichment of PMMA was highly obvious at a low bulk PEO content, but as the bulk PEO content increased, the surface concentration of PEO component increased rapidly and a surface enrichment inversion, i.e. a surface enriched with PEO even occurred. This implies the surface of the copolymers with longer PEO side chains can be completely covered by PEO segments. Forming the higher surface free energy surface may add to it the excellent flexibility and moving ability of the longer PEO side chains. The formation of interface with air may be described as follows:

$$\underset{\text{(between polymer solution and air)}}{\text{Interface}} \xrightarrow{T,\,P} \text{solvent volatilization}$$

$$\underset{\text{(between polymer solid and air)}}{\text{Interface}}$$

As solvents volatilize, polymer molecules are continuously exposed to air and an air–polymer interface gradually forms, PMMA and PEO segments are competitively located on the interface. Thermodynamically, PMMA segments are more likely to be found on the interface than PEO, because PMMA has a lower surface free energy (the surface free energies of PMMA and PEO are 40.2, 44 dyn/cm, respectively). On the other hand, enrichment of PMMA segments

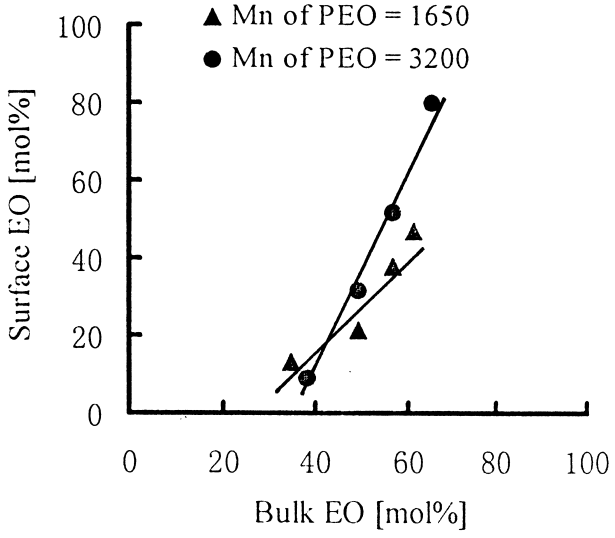


Fig. 2. Surface vs. bulk composition for PMMA-*g*-PEO.

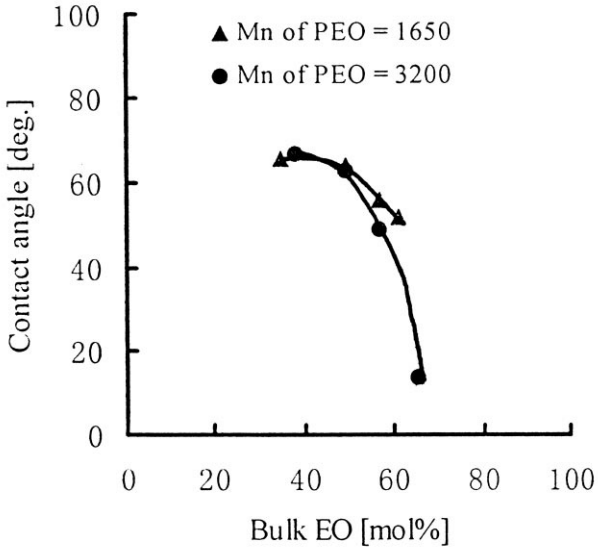


Fig. 3. Static contact angle vs. bulk composition for PMMA-*g*-PEO.

on surface is restricted by some factors such as the bulk composition, the 'installation form' of the two segments (backbone or side chains), and the relative moving ability of the two segments (glass transition temperature, $T_g$). Moreover, because the difference between the surface free energies of PMMA and PEO is small, the thermodynamical impetus to make PMMA segments enrich on surface is not very strong. Because PEO segments are in side chain form and the $T_g$ of PEO is very low, PEO segments have greater flexibility and moving ability than PMMA, and therefore move to the surface more easily. As the bulk concentration of PEO increases, and PEO side chain length increases (the longer the side chain, the greater moving ability PEO segments), less of PMMA segments move to the surface relative to PEO segments.

### 3.1.3. Depth profiling surfaces

The angle-dependent XPS measurements were made by rotating the sample relative to the fixed position electron analyzer and this, in effect, varies the sampling depth. Thus, by taking spectra at angles of $\theta$ ranging from 0 to 60°, one can determine the average composition at certain effective sampling depth and establish a composition-depth profile in the outermost 50 Å of the sample. Table 3 contains the tabulated copolymer compositions at the various sampling depths. A surface decrement of PEO, relative to bulk, was found at all sampling depths and the surface decrement was largest at $\theta = 60°$ where the effective depth is about 25 Å. All of the sample films exhibited a composition gradient over the top 50 Å. This evidence indicates that the PMMA and PEO components in the testing copolymers are both exposed at surface.

Table 3
Mole percent EO at the surface of PMMA-*g*-PEO copolymer films as a function of electron takeoff angle ($\theta$) (effective sampling depth ($d$), nm)

| Sample | $\theta = 0°$; $d = 5.0$ | $\theta = 20°$; $d = 4.7$ | $\theta = 40°$; $d = 3.8$ | $\theta = 60°$; $d = 2.5$ |
|---|---|---|---|---|
| C | 52.7 | 49.1 | 38.2 | 36.0 |
| D | 60.0 | 50.9 | 47.4 | 33.3 |
| F | 17.4 | 14.3 | 9.1 | 6.3 |
| G | 37.0 | 34.6 | 31.9 | 27.3 |

### 3.2. Contact angle

Fig. 3 shows the relationship between static water contact angle ($\theta_s$) and the bulk structural parameters (the bulk composition and PEO side chain length) of the PMMA-*g*-PEO copolymers. For the copolymers with the same PEO side chain length, $\theta_s$ decreased as the bulk PEO content increased; the longer PEO side chains were, the faster $\theta_s$ decreased. If the PEO side chain length factor was not considered, the bulk composition could not be correlated with $\theta_s$; likewise, if the bulk composition factor was not considered, the PEO side chain length also could not be correlated with $\theta_s$. Because $\theta_s$ is only related to the outermost 10 Å of each samples, the surface composition of copolymers is greatly correlated with $\theta_s$. Fig. 4 shows that $\theta_s$ decreased with increasing surface PEO. These results indicate that bulk structural parameters affect $\theta_s$ and surface composition, when $\theta_s$ is small, the sample is more hydrophilic. Therefore, the hydrophilicity of the PMMA-*g*-PEO copolymers can be controlled by adjusting the bulk structural parameters.

The contact angles of water on the copolymer decreased linearly with contact time until they reached a balance value $\theta_e$ or 0. The relationship between $\theta$ and contact time $t$ can be expressed by the following equation: $\theta = -kt$, where $\theta_s < \theta < \theta_e$. It is presumed that the time dependence of $\theta$ is

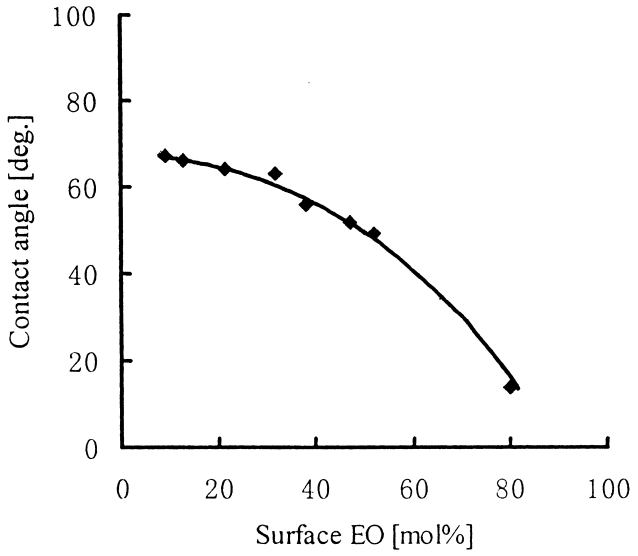


Fig. 4. Static contact angle vs. surface composition for PMMA-*g*-PEO.

affected by the time change of the interfacial tension $\gamma_{SL}$ between PMMA-*g*-PEO copolymers and water.

In general, the contact angle of liquid on solid is expressed by Young's equation:

$$\gamma_L \cos\theta = \gamma_S - \gamma_{SL} - \pi_e$$

where $\gamma_S$ and $\gamma_L$ are the surface tensions of solid and liquid respectively. The spreading pressure $\pi_e$ can be neglected ($\pi_e \ll \gamma_L$). Good and Girifalco [13,14] represented the work of the adhesion $W_a$ as: $W_a = 2\Phi_G(\gamma_S\gamma_L)^{0.5}$, where $\Phi_G$ is the interaction parameter. Ward and Neumann [15] expressed the relationship between $\Phi_G$ and interfacial tension $\gamma_{SL}$ as:

$$\Phi_G = 1 - 0.075\gamma_{SL}$$

Interfacial tension $\gamma_{SL}$ is defined using the above equation and the equation $\Phi_G = (\gamma_S + \gamma_L - \gamma_{SL})/2(\gamma_S\gamma_L)^{0.5}$ as:

$$\gamma_{SL} = (\gamma_S^{0.5} - \gamma_L^{0.5})^2/[1 - 0.15(\gamma_S\gamma_L)^{0.5}]$$

When $\gamma_S = \gamma_L$, the interfacial tension $\gamma_{SL}$ between solid and liquid is a minimum. Therefore, it is presumed that the time dependence of the contact angle occurs by changing the $\gamma_S$ value (rearrangement and orientation of polymer chain) to decrease $\gamma_{SL}$.

Table 4 shows $\theta$ was linearly correlated with contact time $t$, the correlation coefficients were up to 0.99; $k$ and $\Delta\theta$ are measures of structural parameters of polymers. In general, the $\theta_e$ of the PMMA-*g*-PEO copolymers with water was smaller than that of PMMA, and $k$ or $\Delta\theta$ of the PMMA-*g*-PEO copolymers was larger than that of PMMA; for the copolymers with higher PEO component contents or longer PEO side chains or both, $\theta_e$ was smaller and $k$ or $\Delta\theta$ was larger. The static contact angle, $\theta_s$, is usually used to evaluate the surface properties (such as surface tension,wettability or hydrophilicity) of solid polymers in air. $\theta_e$ is the balance contact angle, which is the contact angle after the solid surface contact with water is balanced or in equilibrium. Thus, the surface properties of copolymers in water can in fact be evaluated using $\theta_e$, where $\Delta\theta$ is the variance of this copolymer surface property between air and water, and $k$ is related to the rate of change in surface properties such as $\gamma_S$, i.e. the rate of rearrangement and orientation of the polymer chain. It is not difficult to understand that $k$ and $\Delta\theta$ are related to the bulk structure parameters. Because PMMA has a high $T_g$, and is in the glassy state at the room temperature, rearrangement of PMMA segments cannot occur, only their reorientation can occur; PEO has a very low $T_g$, and is in the highly elastic state at the room temperature. Thus PEO segments can both rearrange and reorient. Compared with PMMA homopolymers, PMMA-*g*-PEO copolymers can more easily change orientation of polymer chains and arrangement of PEO segments. Therefore, the time dependence of contact angle $\theta$ of the PMMA-*g*-PEO copolymers with water is even more obvious. The longer PEO side chains, the greater the hydrophilic PEO segment mobility toward surface contact with water, thus, for the copolymers with longer PEO side chains ($M_n$ of PEO, 3200), $k$ was greater than that of the copolymers with shorter PEO side chains ($M_n$ of PEO, 1650). Because the PEO side chains have greater mobility towards surface in water, the surface PEO content increased and was larger in water than in air.

### 3.3. In vitro blood compatibility assessment

Table 5 shows that the RTs of PMMA-*g*-PEO copolymers were larger than those of PMMA homopolymer or glass, which indicates that PMMA-*g*-PEO copolymers are good blood compatibility. For the copolymers with the same PEO side chain length, as the bulk PEO content increased, the surface PEO content and hydrophilicity increased, RTs increased. This result shows that the ancoagulant activities are closely related to surface PEO contents. This is due to

Table 4
The parameters for the relationship between contact angle ($\theta$) and contact time ($t$)

| Sample | A | B | C | D | E | F | G | H | I | PMMA |
|---|---|---|---|---|---|---|---|---|---|---|
| $\theta_e$ | 50 | 39 | 32 | 25 | 0 | 28 | 0 | 0 | 0 | 61 |
| $\Delta\theta$ | 16 | 25 | 24 | 27 | 26 | 35 | 49 | 14 | 14 | 9 |
| $r$ | 0.989 | 0.995 | 0.983 | 0.995 | 0.990 | 0.997 | 0.995 | 0.997 | 0.982 | 0.973 |
| $k$ | 2.1 | 2.2 | 1.7 | 2.4 | 3.1 | 3.2 | 3.2 | 3.3 | 3.4 | 1.4 |

Table 5
The RT of fresh human platelet-rich plasma on the surfaces of PMMA homopolymer and the PMMA-*g*-PEO copolymers (data are expressed as the mean of six values for each sample ±SE)

| Interface | Glass | PMMA | A | B | C | D | F | G | H | I | J |
|---|---|---|---|---|---|---|---|---|---|---|---|
| With air | 155 ± 7 | 188 ± 8 | 186 ± 9 | 220 ± 7 | 247 ± 9 | 260 ± 13 | 190 ± 8 | 228 ± 9 | 254 ± 12 | 258 ± 12 | 266 ± 13 |
| With water | | | 220 ± 8 | 240 ± 9 | 260 ± 9 | 298 ± 11 | 210 ± 10 | 300 ± 11 | 288 ± 13 | 322 ± 12 | |

the low affinity of PEO for proteins and other blood components, which resists the interaction that lead to thrombus formation at the biomaterial–blood interface [16,17]. PEO has been considered an attractive biocompatible biomaterial because of its ability to resistance of blood components [18,19]. There are influences on RTs of PEO side chain lengths, because surface PEO content depends on both of bulk PEO content and PEO side chain lengths. For the same sample, RT increased after surface water treatment. Water treatment makes surface with air into interface with water, which lead to the increase of surface PEO content due to hydrophilic PEO segment mobility toward surface contact with water. The PMMA-*g*-PEO copolymer film exhibits microphase separated structure which is apparent in Fig. 5 as dark spots due to the binding of $OsO_4$ to PEO segments. $OsO_4$ can bind efficiently to PEO stuctures and be used for contrasting the phases [20]. It was reported that materials having microphase separated structure also showed good blood compatible [21]. However, because there is surface enrichment for the PMMA-*g*-PEO copolymers, their bulk and surface structure may also be different, moreover, their surface composition and morphology may vary with contact media, it is difficult to study the relationship between the microphase structure and the blood compatibility.

## 4. Conclusions

The surface properties of the PMMA-*g*-PEO copolymers were greatly influenced by their bulk composition and graft chain lengths, as well as surface contact media. The copolymer surface was generally enriched with PMMA. However, for the copolymers with long PEO side chains and high bulk PEO component content, a surface enrichment inversion could occur. The contact angles of water on the copolymers decreased linearly with contact time until they reached a balance value $\theta_e$ or 0, and the relationship between $\theta$ (from $\theta_s$ to $\theta_e$) and contact time can be expressed by $\theta = -kt$. $k$ and $\Delta\theta$ depended on the bulk composition and PEO side chain length. The PMMA-*g*-PEO copolymers have good compatibility, which is associated with surface PEO. The PMMA-*g*-PEO copolymers can undergo microphase separation.

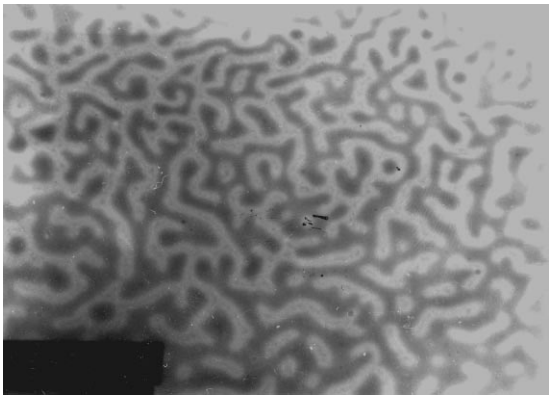

Fig. 5. TEM photograph of thin PMMA-*g*-PEO($M_n$ of PEO = 200, EO = 56.5 mol%) film, contrasted with $OsO_4$. The darkened areas are PEO-rich domains with bound $OsO_4$ (40 360 ×).

## Acknowledgements

Financial support by the National Natural Science Foundation Committee of China and the Anhui Province Natural Science Foundation Committee is gratefully acknowledged.

## References

[1] Kim YJ, Kang I-Y, Huh MW, Yoon S-C. Biomaterials 2000;21:121.
[2] Silver JH, Lin J-C, Lim F, Cooper SL. Biomaterials 1999;20:1533.
[3] Inoue H, Fijimoto K, Uyama Y, Ikada Y. J Biomed Mater Res 1997;35:255.
[4] Nojiri C, Okano T, Jacobs HA, Park KD. J Biomed Mater Res 1990;24:1151.
[5] Park JH, Park KD, Bae YH. Biomaterials 1999;20:943.
[6] Nagaoka S, Nakao A. Biomaterials 1990;11:119.
[7] Fujimoto K, Inoue H, Ikada Y. J Biomed Mater Res 1993;27:1559.
[8] Bergstrom K, Holmberg K, Safranj A, Hoffman AS. J Biomed Mater Res 1992;26:779.
[9] Brinkman E, Poot A, Bantjes A. Biomaterials 1990;11:200.
[10] Walton DG, Soo PP, Mayes AM. Macromolecules 1997;30:6947.
[11] Affrossman S, Kiff T, Pethrick RA. Macromolecules 1999;32:2721.
[12] Lee JH, Kim SK. Polymer-Korea 1997;21:332.
[13] Girifalco LA, Good RJ. J Phys Chem 1957;61:904.
[14] Good RJ, Girifalco LA. J Phys Chem 1960;64:541.
[15] Ward CA, Neumann AW. J Colloid Interface Sci 1974;49:286.
[16] Lee JH, Kopecek J, Andrade JD. J Biomed Mater Res 1989;23:351.
[17] Han DK, Park KD, Ahn KD, Kim YH. J Biomed Mater Res 1989;23:87.
[18] Sheu MS, Hoffman AS, Ratner BD, Feijen J. J Adhesion Sci Technol 1993;7:1065.
[19] Maechling-Strasser C, Dejardin P, Galin JC. J Biomed Mater Res 1989;23:1395.
[20] Kubies D, Rypacek F, Kovarova J. Biomaterials 2000;21:529.
[21] Nojiri C, Okana T. J Biomed Mater Res 1990;24:1151.